Protein Immobilization on Ni(II) Ion Patterns Prepared by Microcontact Printing and Dip-Pen Nanolithography

Chien-Ching Wu,[†,‡] David N. Reinhoudt,[‡] Cees Otto,[†] Aldrik H. Velders,[‡,*] and Vinod Subramaniam[†,*]

[†]Biophysical Engineering Group and [‡]Laboratory of Supramolecular Chemistry and Technology, MESA[+] Institute for Nanotechnology and Faculty of Science and Technology, University of Twente, 7500 AE Enschede, The Netherlands

ABSTRACT An indirect method of protein patterning by using Ni(II) ion templates for immobilization *via* a specific metal—protein interaction is described. A nitrilotriacetic acid (NTA)-terminated self-assembled monolayer (SAM) allows oriented binding of histidine-tagged proteins *via* complexation with late first-row transition metal ions, such as Ni(II). Patterns of nickel(II) ions were prepared on NTA SAM-functionalized glass slides by microcontact printing (μCP) and dip-pen nanolithography (DPN) to obtain micrometer and submicrometer scale patterns. Consecutive dipping of the slides in 6His-protein solutions resulted in the formation of protein patterns, as was subsequently proven by AFM and confocal fluorescence microscopy. This indirect method prevents denaturation of fragile biomolecules caused by direct printing or writing of proteins. Moreover, it yields well-defined patterned monolayers of proteins and, in principle, is indifferent for biomolecules with a high molecular weight. This approach also enabled us to characterize the transfer of Ni(II) ions on fundamental parameters of DPN, such as writing speeds and tip—surface contact times, while writing with the smallest possible ink "molecules" (*i.e.*, metal ions).

KEYWORDS: dip-pen nanolithography (DPN) · self-assembled monolayer (SAM) · microcontact printing (μCP) · fluorescent protein · atomic force microscopy (AFM)

Micro- and nanopatterning of biomolecules on surfaces attracts growing attention due to the potential applications in medicine and biotechnology.[1] Applications include production and preparation of biochips and biosensors for diagnostics, drug discovery, and fundamental studies of biological processes.[1,2] Different techniques have been developed to accomplish biopatterning at the micro- and nanoscale, such as soft lithography,[3−5] scanning probe lithography,[6−11] nanoimprint lithography,[12−14] and electron beam lithography.[15−17] We have previously demonstrated that metal ions can be transferred onto fluorescent SAMs using microcontact printing (μCP) and dip-pen nanolithography (DPN) with micrometer and submicrometer precision.[18] Subsequent modulations of fluorescent signals were visualized *in situ* by using a hybrid atomic force fluorescence microscope (AFFM).[18,19] A potential application of metal ion patterns is their use as a template for selective and controlled immobilization of biomolecules *via* a specific metal−protein interaction.[20,21]

Nickel(II) nitrilotriacetic acid (Ni-NTA) is used in metal affinity chromatography (IMAC) for purifying proteins labeled with a short sequence of histidines.[22] This Ni-NTA system has also been adopted for fabricating biomolecule patterns on surfaces[8,11,12,23−25] due to the high affinity ($K_d \approx 10^{-13}$ M) of the 6His-tag to Ni-NTA[26] and the oriented and reversible binding of His-tagged biomolecules *via* the formation of complexes with Ni(II) ions (or other metal ions such as Cu(II) or Co(II)).[12] However, to the best of our knowledge, directly fabricating patterns of metal ions with lithographic techniques as a template for immobilization of proteins has not been reported. In this paper, we have used NTA-terminated SAMs (NTA SAMs) on glass substrates to prove this concept.

In early experiments, we have used microcontact printing (μCP) to fabricate micrometer scale nickel(II) ion patterns onto NTA SAM-functionalized glass slides because of the simplicity and high-throughput production of the μCP technique.[3] The metal ion patterned substrates were incubated immediately with His-tagged protein solutions to anchor the proteins onto the printed areas. Subsequently, we have utilized the AFFM to perform dip-pen nanolithography (DPN), a high-resolution patterning technique,[9,10,27] to scale down the size of nickel ion patterns to the submicrometer scale, accompanied by direct visualization of the results by AFM and fluorescence microscopy. Using metal ion patterns as a template is an indirect approach to fabricate protein patterns, with the advantage that denaturation of fragile biomolecules

*Address correspondence to v.subramaniam@tnw.utwente.nl, a.h.velders@utwente.nl.

Received for review September 22, 2009 and accepted January 21, 2010.

Published online January 27, 2010.
10.1021/nn901270c

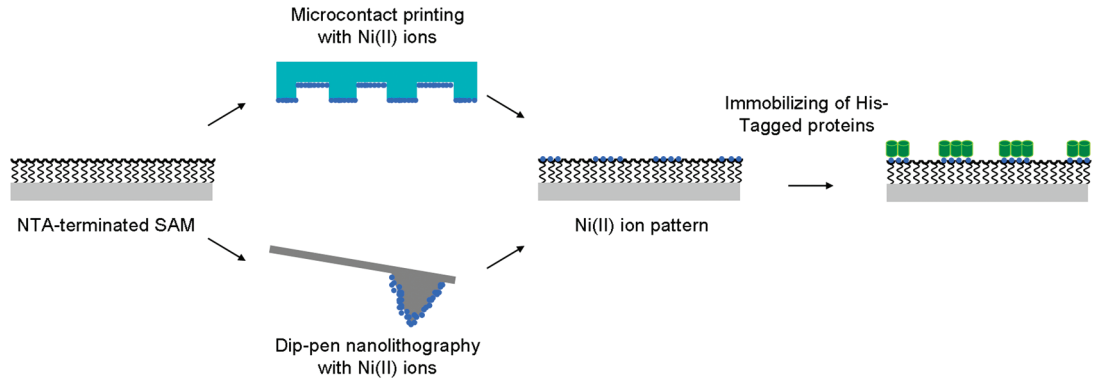

Figure 1. Fabrication of Ni(II) ion patterns onto NTA-terminated SAM with microcontact printing (μCP) and dip-pen nanolithography (DPN) to immobilize His-tagged proteins.

readily observed when printing or writing proteins directly is avoided.[28] Enhanced green fluorescent protein incorporating a 6His-tag (His-EGFP) was used as a model protein. EGFP is intrinsically fluorescent when properly folded and thus can be directly used for optical recognition. The intrinsic fluorescence is also a marker of the structural integrity of the protein; misfolded or otherwise structurally damaged proteins do not fluoresce. The AFFM enables both fabrication of nickel(II) ion patterns and *in situ* observation of the fluorescence and atomic force microscopy (AFM) topography of the protein patterns. AFM measurements provide a better determination of the real size of protein patterns as it surpasses the resolution limitation of confocal fluorescence microscopy. Despite the difference in sizes of the proteins and the intermediate metal ions, fluorescence and topographic results of the protein patterns enabled us to better characterize the transfer and diffusion on the surface of Ni(II) ions as a function of fundamental parameters of DPN, such as writing speeds and tip−surface contact times. In a further demonstration of the general applicability of this method, we have also patterned a higher molecular weight histidine-tagged protein, the tetrameric reef coral fluorescent protein (His-DsRed).

RESULTS AND DISCUSSION

The procedure of fabricating protein patterns by using metal ion patterns as a template is illustrated in Figure 1. Ni(II) ions were first printed with microcontact printing (μCP) or deposited with dip-pen nanolithography (DPN) onto the NTA-terminated SAM. Subsequently, the metal ion patterned substrates were incubated with His-tagged protein solutions to anchor the proteins onto the printed areas. Since the metal ion pattern itself is difficult to visualize directly, development with His-tagged visible fluorescent proteins (VFPs) enables a further investigation of fundamental aspects of the DPN process, such as the effects of varying tip−surface contact times at fixed positions and writing speeds.

Fabrication of His-EGFP Patterns by Microcontact Printing (μCP). Microcontact printing is an easy and fast approach to prove that Ni(II) ion patterns on NTA surfaces can be used as templates for the immobilization of His-tagged proteins at the micrometer scale. A PDMS stamp with 5 μm line features, with a spacing of 3 μm, was coated with Ni(II) ions and brought into conformal contact with the NTA-modified surface for a contact time of 3 min before incubating the latter in a 100 nM His-EGFP solution. In Figure 2a, the fluorescence image of a patterned surface shows His-EGFP areas with the expected feature size of the microcontact printed Ni(II) ion pattern, illustrating that His-EGFP patterns can be readily obtained by this indirect method of using Ni(II) ions as templates.

We have previously reported that His-tagged proteins complexed on Ni(II)-NTA SAMs can be easily removed by EDTA solution for reusing the functionalized substrates.[12] To demonstrate that our functionalized surfaces are reusable, a substrate with a His-EGFP pattern was incubated in an 0.1 M EDTA solution overnight and then rinsed with water and 10 mM Tris-HCl buffer (pH 8). Figure 2b shows that there are no apparent fluorescent features on the substrate after it was treated with EDTA solution. A PDMS stamp with a different feature size (10 μm line features, separated by 5 μm) was used for a second microcontact printing of Ni(II) ions on the regenerated slide. Figure 2c shows that His-EGFP was successfully attached onto reprinted Ni(II) ion patterns, confirming that the NTA-functionalized surface can be effectively reutilized. The slight difference in fluorescence intensities between panels a and c of Figure 2 may result from the difference in the amount of Ni(II) ions adsorbed onto the surfaces of the different PDMS stamps used.

Fabrication of His-EGFP Patterns by Dip-Pen Nanolithography (DPN). We explored the fabrication of submicrometer scale metal ion patterns on NTA SAM-functionalized glass by DPN, a technique which is more flexible and can create patterns with smaller feature sizes than μCP.[27] DPN can also modify the surface with different inks, whereas μCP is normally a single ink process. We

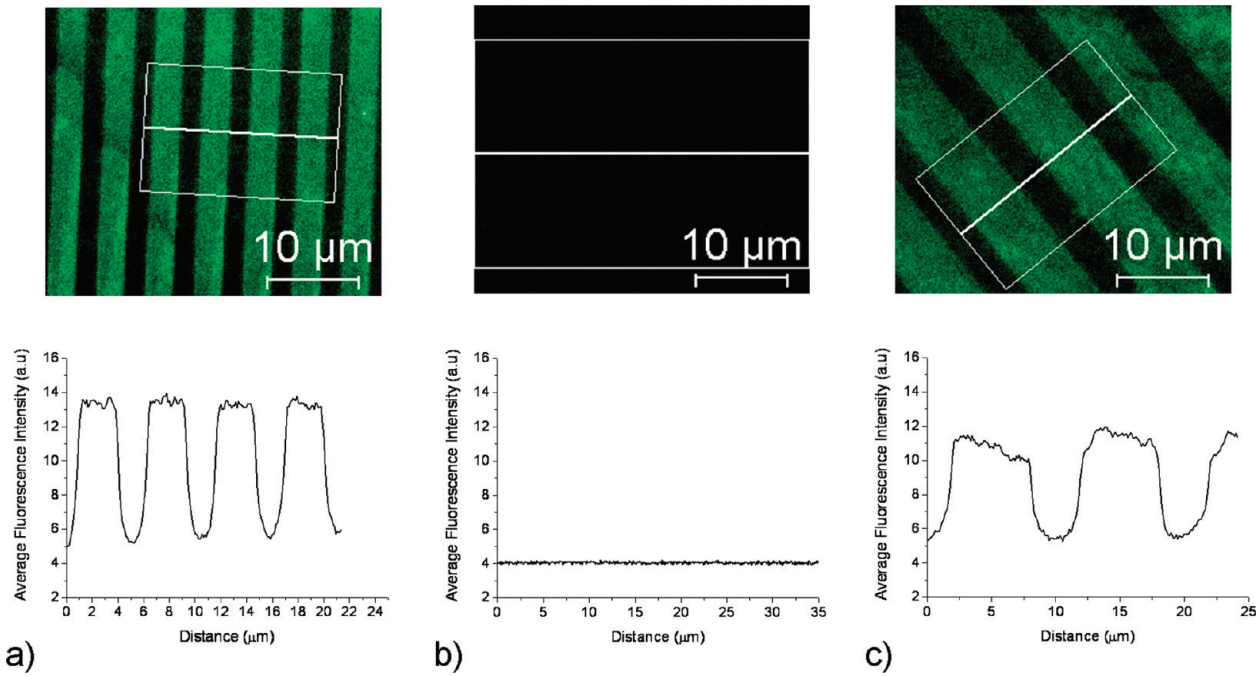

Figure 2. Fluorescence images and average fluorescence intensity profiles of the area inside the rectangle of His-EGFP immobilized on Ni(II) patterns created after (a) first μCP of 5 μm line features, (b) after rinsing with 0.1 M EDTA solution, and (c) after second μCP of 10 μm line features. The exposure time of the camera for each of the images is the same.

fabricated metal ion patterns with DPN, followed by protein incubation, and subsequently monitored fluorescence and AFM topography *in situ* with the AFFM. The use of this hybrid instrument avoids the intrinsic difficulty of finding the written protein patterns after transferring the sample from the AFM to a fluorescence microscope. For the purpose of scaling down the size of Ni(II) ion patterns, a cleaned Si_3N_4 AFM tip was inked with Ni(II) ions by dipping into a $NiCl_2$ solution, and the ink-loaded tip was brought into contact with an NTA-functionalized surface for writing dot or line patterns directly above the central focus of the objective lens. The driving forces for the transfer of Ni(II) ions from an AFM tip to a surface are the dissolution of metal ions into the aqueous meniscus formed between tip and surface and the complex formation of Ni(II) ions with NTA molecules functionalized on the glass substrates. The written Ni(II) ion patterns were then immersed in a protein solution and consecutively visualized by fluorescence microscopy (Figures 3a, 5a, and 7b).

Metal ions are among the smallest ink "molecules" one can use. It is very difficult to directly characterize the transferred Ni(II) ions on a surface because of the small size of the ions. However, the amount of transfer of Ni(II) ions can be revealed by the subsequent immobilization of His-EGFP and measurement of its intrinsic fluorescence, allowing the systematic investigation of metal ion deposition by DPN. Therefore, DPN experiments were carried out, in which either an ink-coated AFM tip was held at different fixed positions for different times (dot patterns) or the AFM tip was moved at different, but constant, writing speeds (line patterns).

Writing with Different Contact Times. A Ni(II) ion pattern of 18 dots was written with different tip−surface contact times for each dot, varying between 1 and 60 s. The tip was brought into contact with the surface for a given time and was retracted after writing each dot. The contact time was monotonically increased, and the whole writing sequence was completed without reinking the tip. The written area was immediately incubated in a 100 nM His-EGFP solution for 30 min and then rinsed with 10 mM Tris-HCl buffer (pH 8) and Milli-Q water before drying with N_2. The fluorescence image of the His-EGFP dot patterns is shown in Figure 3a. The observed His-EGFP dot patterns are consistent with the written Ni(II) ion patterns, which indicates Ni(II) ions have been transferred from the AFM tip onto the surface. To elucidate the relationship between the fluorescence intensity and tip−surface contact time, the fluorescence intensities of 32 × 32 pixels covering each dot were averaged. It is known that there is a correlation between the tip−substrate contact time and the amount of deposited ink molecules.[9,27,29] Normally, longer contact times between the tip and the substrate on a certain area, or using slower scanning speeds, should result in higher amount of ink transferred to the substrate. In Figure 3a, dots deposited for longer times show higher fluorescence intensity, indicating that more His-EGFP molecules were attached to the written area. In Figure 3b, a plot of the averaged fluorescence intensities *versus* the tip−surface contact time shows a linear relationship, suggesting that the amount of Ni(II) ions trans-

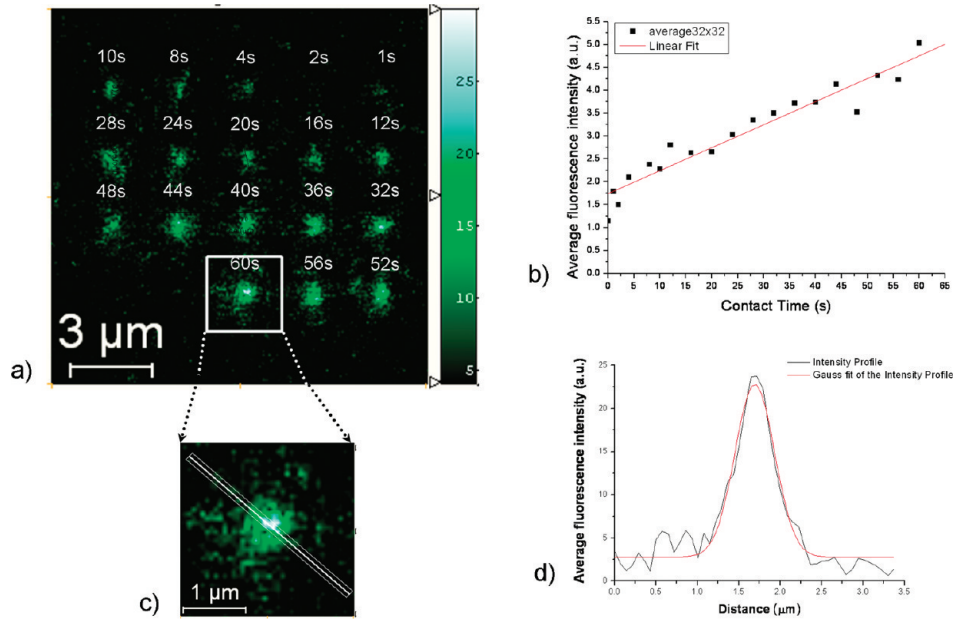

Figure 3. (a) Fluorescence images of His-EGFP patterns acquired after incubating slides with deposited metal ion areas with the protein solution. The dot patterns were successively generated by using an AFM tip inked with Ni(II) ion using tip−surface contact times listed above the dot patterns. The exposure time used for obtaining the images was 0.25 ms per pixel. (b) Plot of average fluorescence intensity of each dot within 32 × 32 pixel region around the dot *versus* tip−surface contact time. The intensity with a contact time of 0 s was obtained by averaging a 32 × 32 pixel area which was not in contact with the ink-coated tip; the observed fluorescence can be attributed to the nonspecific binding effect of protein on NTA-functionalized surface. A linear fit to the data is plotted in red. (c) Zoom-in of His-EGFP dot pattern written with tip−surface contact time of 60 s shown in panel a. (d) Average fluorescence intensity profile of the area inside the rectangle indicated in c (black line) and its Gaussian fit profile (red line).

ferred onto the NTA-functionalized surface increases linearly with the tip−surface contact time.

One important factor in determining the resolution in DPN experiments is how ink molecules diffuse from a tip to a surface *via* a water meniscus.[30] Our DPN experiments were operated at ~60% relative humidity (RH), and it has been reported that, at this RH, a water meniscus of ~1.5 μm in diameter is formed between tip and substrate.[31] The size of the water meniscus may suggest that the maximum size of the Ni(II) ion spot and its corresponding His-EGFP pattern is also ~1.5 μm in diameter. The diameters of His-EGFP dot patterns written with tip−surface contact times longer than 10 s shown in Figure 3a are in fact between ~1.0 and ~ 1.4 μm. Besides, a gradient in fluorescence intensity was observed; that is, each dot exhibits higher emission in the center and a lower emission at the borders. One example is exhibited in Figure 3c, which is the enlargement of the fluorescent dot pattern written with a tip−surface contact time of 60 s. The average fluorescence intensity profile (Figure 3d) of the area inside the rectangle as indicated in Figure 3c clearly highlights the gradient of fluorescence intensity. This profile can be fit well with a Gaussian function, which suggests that the gradient phenomenon may be attributed to the radial diffusion of the nickel ions from the contact position of tip and surface to the border of the spot (see Supporting Information Figure S1 for a plot of full width at half-maximum values of intensity profiles of each spot in Figure 3a as a function of the tip−surface contact times).

AFM imaging reveals topographic information of the protein patterns adhered to metal ion sites. To avoid contaminations, a new Si_3N_4 AFM tip was brought to the original position in the DPN experiments, directly above the central focus of the objective lens. The topography measurements were performed in tapping mode and are shown in Figure 4a. The 18-dots protein pattern shown in the AFM height image corresponds well to the pattern in the fluorescence image. It can be observed that the spots with higher fluorescence intensity have more distinct AFM patterns, suggesting the denser packing of His-EGFP. The diameters of these more densely packed protein dots are between ~300 and ~800 nm. The height profile of protein patterns generated with the tip−surface time of 10, 28, and 48 s is shown in Figure 4b. The reported size of EGFP in the literature is a cylinder of ~2 nm in diameter and ~4 nm in height.[32] Figure 4b indicates that a monolayer of protein patterns was achieved.

Writing at Varying Speeds. We were also able to successfully generate line patterns by fabricating Ni(II) ion patterns as a template. A Ni(II) ion pattern of five 10 μm long lines with five different scan speeds varying between 10 and 0.1 μm s^{-1} was written. Each line was scanned once, and the tip was retracted after finishing each line. The same tip was used without reinking to fabricate a second, identical, five-line pattern. The writ-

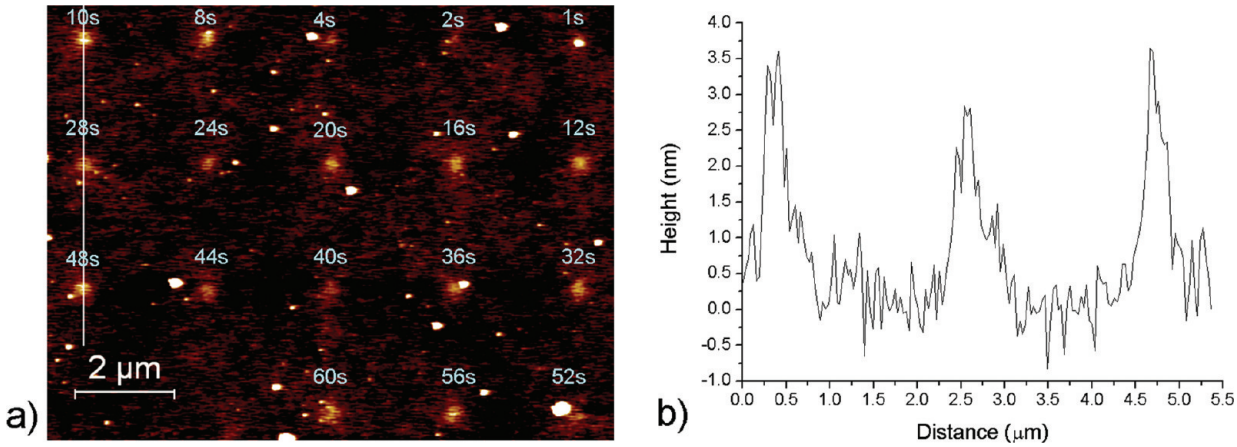

Figure 4. (a) AFM tapping mode height image of His-EGFP attached to Ni(II) ion patterns fabricated with dip-pen nanolithography. Some (white) spots shown in the image may result from dust particles or dried salt crystals from the buffer solution. (b) Height profile of protein dots generated with tip−surface contact times of 10, 28, and 48 s (from left to right).

ten area was incubated with a His-EGFP solution to develop the Ni(II) ion pattern. The fluorescence image of the fabricated His-EGFP lines is shown in Figure 5a. We again observe that the protein line patterns correspond to the designed metal ion patterns. A gradient, in-plane and orthogonal to the writing direction, in the fluorescence intensity could also be observed in the line patterns, suggesting that a similar diffusion of Ni(II) ions takes places as observed in the dot patterns. Figure 5b shows the average fluorescence intensity profiles of each line in the first five-line pattern which were fit well with Gaussian functions. The lines with higher fluorescence intensity have more distinct AFM line patterns with a line width of ~700 nm. The corresponding AFM tapping mode height image of the His-EGFP line pattern is exhibited in the accompanying Supporting Information (Figure S2).

The relationship between the amount of deposited Ni(II) ions and scanning speeds derived by measuring the average fluorescence intensity of each line *versus* writing speed is shown in Figure 6a. Comparing the average fluorescence intensities of these two five-line patterns, we note that the lines written with lower speeds in the first five-line pattern have slightly higher fluorescence intensity than the ones in the second five-line pattern. This decrease of fluorescence intensity might result from the depletion of Ni(II) ions coated on the AFM tip surface while performing DPN experiments

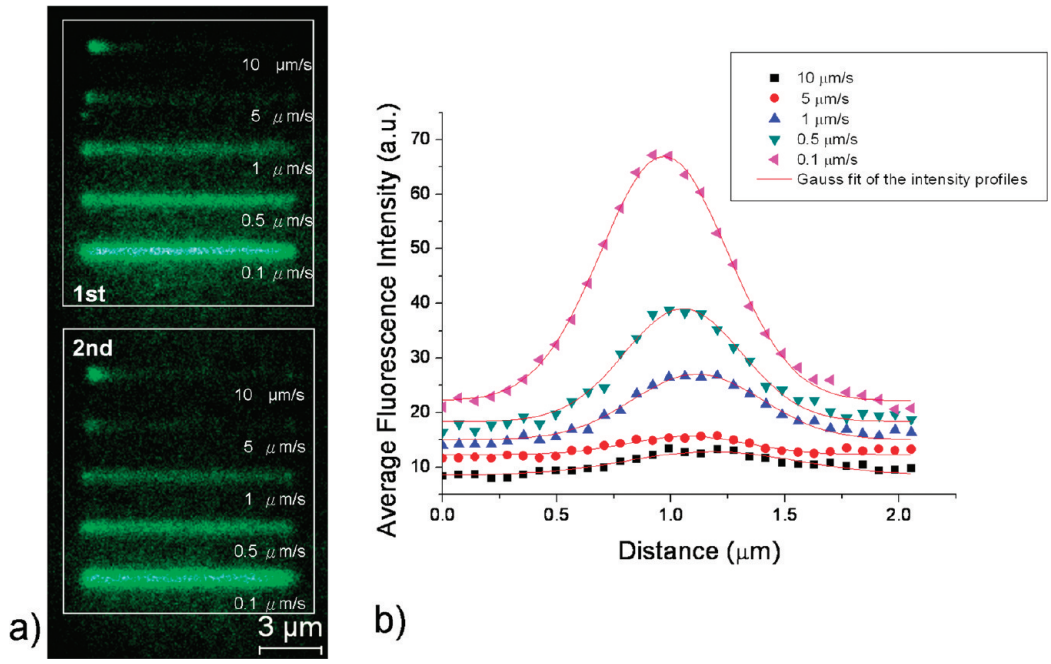

Figure 5. (a) Fluorescence images of His-EGFP patterns acquired after incubating metal ion written areas with protein solution. The upper five-line pattern was written first. The pattern includes five horizontal lines (10 μm in length) that were successively generated by using an AFM tip inked with Ni(II) ions, using scanning speeds of 10, 5, 1, 0.5, and 0.1 μm s^{-1}, from top to bottom. The camera exposure time for these images is 0.25 ms per pixel. (b) Average fluorescence intensity profiles and Gaussian fit (in red) of each line in the first five-line pattern.

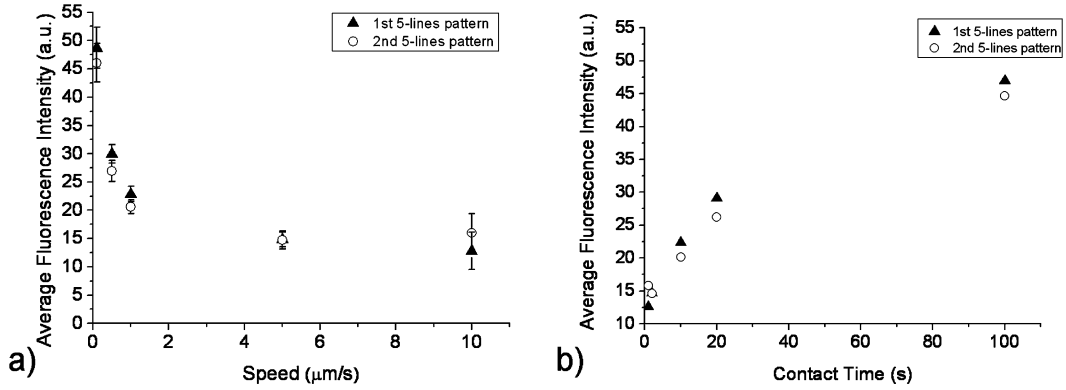

Figure 6. (a) Average fluorescence intensities of each line *versus* the writing speeds. (b) Plot of average fluorescence intensity of each line within 142 × 14 pixels (~10 μm in length and ~1 μm in width) in panel a *versus* tip−surface contact time.

continuously, that is, without reinking. From Figures 5 and 6a, it is clear that Ni(II) ion lines written at a lower scanning rate show higher fluorescence intensity, which indicates that more His-EGFP molecules were attached to the written area. To convert the relation between the fluorescence intensity *versus* writing speed to the fluorescence intensity *versus* tip−surface contact time, the fluorescence intensities over the area of each line (142 × 14 pixels) were averaged. The tip−surface contact time is the time taken to finish the scan of one line. Figure 6b shows the average fluorescence intensity *versus* tip−surface contact time of these two five-line patterns. A close to saturation fluorescence intensity was observed while depositing Ni(II) ions with the slowest scanning speed. A similar result has been reported by Deng *et al.*, observing the saturation of fluorescence emitted from 6His-GFP when the Cu(II) ion density on polyether-functionalized glass substrates is more than ~1.5×10^{14} cm^{-2}.[33]

It is interesting to notice the difference between Figure 3b (steady state) and Figure 6b (writing), although the values of the fluorescence intensity in these two figures are not easily compared with each other due to different experimental conditions. Figure 6b shows that the average fluorescence intensity saturates gradually, while the average fluorescence intensity in Figure 3b does not show a tendency to saturate even after depositing Ni(II) ions for 60 s. This difference is probably due to the different amounts of Ni(II) ions on the tip surface at the beginning of DPN experiments. There are practical difficulties in reproducibly creating different tips with the same amount of Ni(II) ions. To allow a more thorough investigation of the fundamental DPN parameters, it would be useful to overcome the ink depletion and imperfect coating of ink molecules, for example, by exploiting fountain pen nanolithography[34] or functionalized tip surfaces[35] as an alternative approach for future experiments.

Fabrication of His-DsRed Patterns by μCP and DPN. We have utilized His-EGFP to demonstrate successfully that proteins can be immobilized onto metal ion templates fabricated with μCP and DPN. To further demonstrate the general applicability of this method, we have also patterned tetrameric reef coral fluorescent protein incorporating a His-tag (His-DsRed). Figure 7a,b shows that His-DsRed was attached well onto the Ni(II) ion patterns fabricated by μCP and DPN, respectively. A tapping mode AFM topography image of the region displayed in Figure 7b is shown in Figure 7c. From the cross section profile of the AFM height image (Figure 7d), it can be seen clearly that the line width and height of the His-DsRed line pattern are ~400 and ~4 nm, respectively. The AFM topographic information again demonstrates the formation of a monolayer of pro-

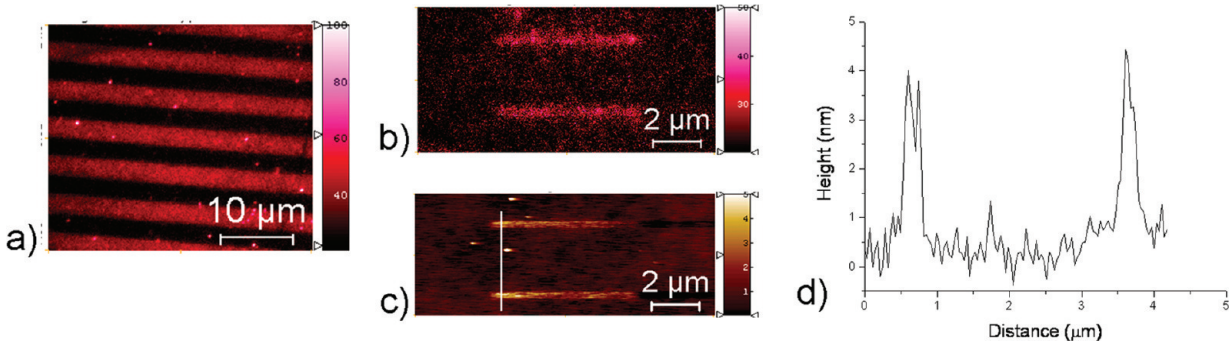

Figure 7. Fluorescence images of His-DsRed immobilized on Ni(II) ion pattern created by (a) microcontact printing and (b) dip-pen nanolithography. (c) AFM tapping mode height image of panel b. (d) Cross section profile of His-DsRed line pattern shown in panel c.

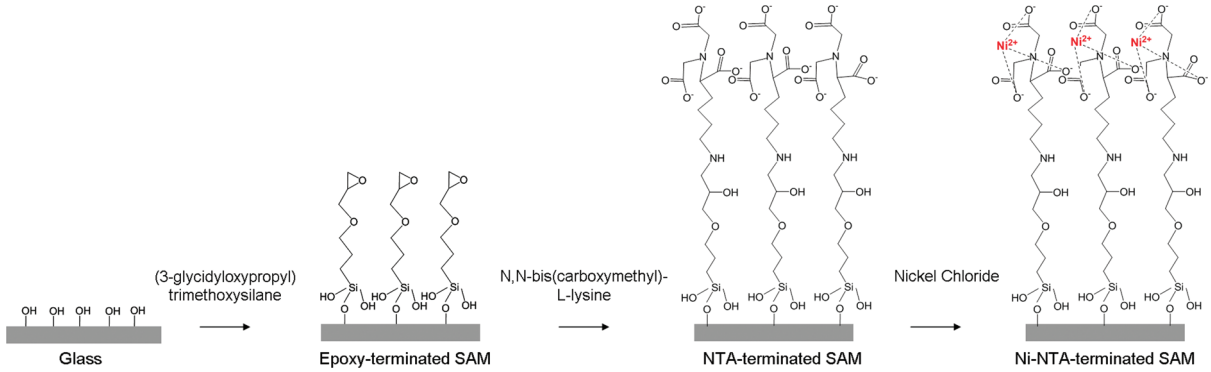

Figure 8. Scheme of fabrication of Ni-NTA-terminated SAMs.

teins. In principle, the indirect writing method puts no limits regarding the molecular weight of the molecule (*e.g.*, protein) to be immobilized, which offers an important flexibility and advantage as a patterning technique.

In general, the approach of using DPN to write metal ions gives us the possibility to reuse the NTA substrate by stripping the patterned metal ions and repatterning with arbitrary geometries, and it may further provide the possibility to generate multiple protein patterns, for example, using EDTA to selectively remove some regions of preimmobilized proteins and then backfilling with another kind of His-tagged protein.

CONCLUSIONS

In summary, we have developed a general method of fabricating Ni(II) ion patterns on NTA SAM-functionalized glass substrates as templates for the immobilization of His-tagged biomolecules at micrometer and submicrometer scale by microcontact printing or dip-pen nanolithography. The advantage of this method is that it allows the oriented and reversible attachment of biomolecules while avoiding protein denaturation because no direct printing or writing of biomolecules is needed. Moreover, this method furnishes well-defined single-molecule layers. The main driving force for the transfer of material from a PDMS stamp or an AFM tip to a substrate is the formation of complexed Ni(II) onto the NTA-functionalized monolayer on glass substrates. The smallest size in diameter or width of His-EGFP or His-DsRed patterns that we can presently achieve by using DPN is around 400 nm. This indirect approach is, in principle, capable of fabricating multiple protein patterns, experiments which are currently underway. We have used a hybrid atomic force and fluorescence microscope to perform direct write−read DPN experiments and obtained *in situ* fluorescence images and AFM topography information of the fabricated patterns. By utilizing the intrinsic fluorescence property of His-EGFP, we could study the relationship between tip−surface contact time and deposited amount of Ni(II) ions.

EXPERIMENTAL METHODS

General Procedures. All glassware used to prepare the monolayers was cleaned by sonicating for 60 min in a 2% v/v Hellmanex II solution in high purity water (Milli-Q, 18.2 MΩcm) and then rinsed thoroughly with Milli-Q water and dried in an ambient environment. Microscope glass slide substrates were cleaned in piranha solution for 20 min (concentrated H_2SO_4 and 33% aqueous H_2O_2 in a 3:1 ratio). [Warning: Piranha solution should be handled with caution: it has been reported to detonate unexpectedly.] The glass slides were then rinsed several times with Milli-Q water and dried gently under a nitrogen stream before forming the monolayer.

NTA and Ni-NTA Monolayer Preparation. The NTA monolayer was prepared by following the procedures reported by Paik *et al.*[36] The freshly cleaned substrates were immersed into a distilled toluene solution containing 1% (v/v) 3-glycidyloxypropyl trimethoxysilane under argon for 2 days. After the substrates were removed from the solution, they were rinsed with distilled toluene and dried under a nitrogen stream. The substrates functionalized with epoxy-terminated SAM were incubated in 10 mM Tris-HCl buffer (pH 8.0) containing 2.5 mM *N,N*-bis(carboxymethyl)-L-lysine (NTA) at 60 °C for 4 h. The substrates were rinsed with Milli-Q water and dried in preparation for μCP and DPN experiments. Ni-NTA surfaces were obtained by immersing the NTA-functionalized substrates into 10 mM Tris-HCl buffer (pH 8.0) containing 0.1 M $NiCl_2$ for 30 min. They were then rinsed several times with Milli-Q water and dried under a nitrogen stream. The scheme of SAM fabrication is shown in Figure 8. The formation of the monolayers was examined by water contact-angle goniometry and ellipsometry. The results are consistent with the values reported in the literature.[12,37] The theoretical value of NTA SAM density is $\sim 6 \times 10^{14}$ molecules $\cdot$ cm^{-2}, which suggests that the maximum density of Ni(II) ions will have a similar value.[38] A limited nonspecific binding effect of His-tagged protein to the NTA SAM was observed (see details in Supporting Information Figure S3). However, there is sufficient fluorescent contrast between Ni-NTA SAM and NTA SAM when His-EGFP is used to develop the pattern, showing the NTA SAM to be a suitable surface for fabricating Ni(II) ion patterns with microcontact printing and dip-pen nanolithography techniques.

Microcontact Printing (μCP). A 10:1 (v/v) mixture of poly(dimethylsiloxane) (PDMS) and curing agent (Sylgard 184, Dow Corning) was cast against a patterned silicon master to prepare PDMS stamps with 5 μm line features, with a spacing of 3 and 10 μm line features and a spacing of 5 μm. The nonoxidized PDMS stamps were incubated in 10 mM Tris-HCl buffer (pH 8.0) containing 0.1 M $NiCl_2$ for ∼1 h and then dried with a nitrogen stream. The stamps were brought into contact with a NTA-terminated substrate for 3 min. After peeling off the stamp, the Ni(II)-printed substrates were incubated in ∼ 200 μL of 25 mM Tris-HCl buffer (pH 7.5) containing 100 nM of His-EGFP or His-DsRed for 30 min and then rinsed

with 10 mM Tris-HCl buffer (pH 8.0) and Milli-Q water to remove excess protein. The substrates with protein patterns were dried under a nitrogen stream before imaging with a fluorescence microscope (TE2000, Nikon).

Dip-Pen Nanolithography (DPN) and Visualization with AFFM. A custom-built atomic force fluorescence microscope (AFFM) described in detail by Kassies *et al.*[19] was used to perform dip-pen nanolithography and to observe the results of patterning *in situ* without having to change to another instrument. Commercial Si_3N_4 AFM cantilevers (Veeco Probes) with nominal spring constant of 0.54 N m^{-1} were used. Immediately before a DPN experiment, the cantilever was rinsed rigorously with ethanol and dried under a stream of N_2. Cleaned cantilevers were then immersed into 10 mM Tris-HCl buffer (pH 8.0) containing 0.1 M $NiCl_2$ for at least 15 min and dried with N_2. The Ni(II) ion coated cantilever was mounted on the AFM head and used to carry out DPN experiments on NTA SAM substrates in contact mode inside a custom-built chamber with a controlled humidity (~60%) at a temperature between 20 and 22 °C.[18,39] The force applied by the AFM tip on the substrate was adjusted between 30 and 50 nN in all experiments to avoid damage of the fluorescent SAMs. Immediately after DPN, ~5 μL of 100 nM His-EGFP or His-DsRed solution was placed onto the written area for 30 min and rinsed with 10 mM Tris-HCl buffer (pH 8.0) and water to remove excess protein. Before fluorescence imaging of the DPN patterns, the substrate was carefully dried with a N_2 stream *in situ* to avoid displacement of the patterned area from the observation range of the objective. The His-EGFP and His-DsRed patterns were excited with the 488 nm line of an argon ion laser (163-D Laser System, Spectra Physics), and the emission of the fluorescence was recorded by an avalanche photodiode (APD) (SPCM-AQR-14, Perkin-Elmer Optoelectronics). The original ink-coated tip was replaced by a new Si_3N_4 AFM tip to prevent contamination of the patterned areas during subsequent imaging. AFM tapping mode was used to obtain topographic information of the protein patterns. Fluorescence and topographic images were analyzed and prepared with the commercial software SPIP (Image Metrology, version 4.4.3.0).

Acknowledgment. We thank K. van der Werf, A. Lenferink, and M. Bennink for their kind help on the AFFM setup, and F. Costantini for generously sharing knowledge of preparing the monolayers. This work was supported by the MESA$^+$ Institute for Nanotechnology and NanoNed.

Note added after ASAP publication: A corrected version of Figure 8 was posted with the issue on February 23, 2010.

Supporting Information Available: Figure S1: Plot of full width at half-maximum values of intensity profiles of each spot in Figure 3a as a function of the tip−surface contact times. Figure S2: Fluorescence and AFM tapping mode height images of line patterns generated by DPN. Experimental details of nonspecific binding effect of NTA-SAM and corresponding image (Figure S3). This material is available free of charge *via* the Internet at http://pubs.acs.org.

REFERENCES AND NOTES

1. Christman, K. L.; Enriquez-Rios, V. D.; Maynard, H. D. Nanopatterning Proteins and Peptides. *Soft Matter* **2006**, *2*, 928–939.
2. Mendes, P. M.; Yeung, C. L.; Preece, J. A. Bio-Nanopatterning of Surfaces. *Nanoscale Res. Lett.* **2007**, *2*, 373–384.
3. Weibel, D. B.; DiLuzio, W. R.; Whitesides, G. M. Microfabrication Meets Microbiology. *Nat. Rev. Microbiol.* **2007**, *5*, 209–218.
4. Kane, R. S.; Takayama, S.; Ostuni, E.; Ingber, D. E.; Whitesides, G. M. Patterning Proteins and Cells Using Soft Lithography. *Biomaterials* **1999**, *20*, 2363–2376.
5. Li, H. W.; Muir, B. V. O.; Fichet, G.; Huck, W. T. S. Nanocontact Printing: A Route to Sub-50-nm-Scale Chemical and Biological Patterning. *Langmuir* **2003**, *19*, 1963–1965.
6. Nam, J. M.; Han, S. W.; Lee, K. B.; Liu, X. G.; Ratner, M. A.; Mirkin, C. A. Bioactive Protein Nanoarrays on Nickel Oxide Surfaces Formed by Dip-Pen Nanolithography. *Angew. Chem., Int. Ed.* **2004**, *43*, 1246–1249.
7. Kenseth, J. R.; Harnisch, J. A.; Jones, V. W.; Porter, M. D. Investigation of Approaches for the Fabrication of Protein Patterns by Scanning Probe Lithography. *Langmuir* **2001**, *17*, 4105–4112.
8. Kim, K. H.; Kim, J. D.; Kim, Y. J.; Kong, S. H.; Jung, S. Y.; Jung, H. Protein Immobilization without Purification *via* Dip-Pen Nanolithography. *Small* **2008**, *4*, 1089–1094.
9. Ginger, D. S.; Zhang, H.; Mirkin, C. A. The Evolution of Dip-Pen Nanolithography. *Angew. Chem., Int. Ed.* **2004**, *43*, 30–45.
10. Salaita, K.; Wang, Y. H.; Mirkin, C. A. Applications of Dip-Pen Nanolithography. *Nat. Nanotechnol.* **2007**, *2*, 145–155.
11. Tinazli, A.; Piehler, J.; Beuttler, M.; Guckenberger, R.; Tampe, R. Native Protein Nanolithography That Can Write, Read and Erase. *Nat. Nanotechnol.* **2007**, *2*, 220–225.
12. Maury, P.; Escalante, M.; Peter, M.; Reinhoudt, D. N.; Subramaniam, V.; Huskens, J. Creating Nanopatterns of His-Tagged Proteins on Surfaces by Nanoimprint Lithography Using Specific NiNTA-Histidine Interactions. *Small* **2007**, *3*, 1584–1592.
13. Falconnet, D.; Pasqui, D.; Park, S.; Eckert, R.; Schift, H.; Gobrecht, J.; Barbucci, R.; Textor, M. A Novel Approach to Produce Protein Nanopatterns by Combining Nanoimprint Lithography and Molecular Self-Assembly. *Nano Lett.* **2004**, *4*, 1909–1914.
14. Escalante, M.; Zhao, Y. P.; Ludden, M. J. W.; Vermeij, R.; Olsen, J. D.; Berenschot, E.; Hunter, C. N.; Huskens, J.; Subramaniam, V.; Otto, C. Nanometer Arrays of Functional Light Harvesting Antenna Complexes by Nanoimprint Lithography and Host−Guest Interactions. *J. Am. Chem. Soc.* **2008**, *130*, 8892–8893.
15. Hong, Y.; Krsko, P.; Libera, M. Protein Surface Patterning Using Nanoscale PEG Hydrogels. *Langmuir* **2004**, *20*, 11123–11126.
16. Rundqvist, J.; Hoh, J. H.; Haviland, D. B. Directed Immobilization of Protein-Coated Nanospheres to Nanometer-Scale Patterns Fabricated by Electron Beam Lithography of Poly(ethylene Glycol) Self-Assembled Monolayers. *Langmuir* **2006**, *22*, 5100–5107.
17. Christman, K. L.; Schopf, E.; Broyer, R. M.; Li, R. C.; Chen, Y.; Maynard, H. D. Positioning Multiple Proteins at the Nanoscale with Electron Beam Cross-Linked Functional Polymers. *J. Am. Chem. Soc.* **2009**, *131*, 521–527.
18. Basabe-Desmonts, L.; Wu, C. C.; van der Werf, K. O.; Peter, M.; Bennink, M.; Otto, C.; Velders, A. H.; Reinhoudt, D. N.; Subramaniam, V.; Crego-Calama, M. Fabrication and Visualization of Metal-Ion Patterns on Glass by Dip-Pen Nanolithography. *ChemPhysChem* **2008**, *9*, 1680–1687.
19. Kassies, R.; Van der Werf, K. O.; Lenferink, A.; Hunter, C. N.; Olsen, J. D.; Subramaniam, V.; Otto, C. Combined AFM and Confocal Fluorescence Microscope for Applications in Bio-Nanotechnology. *J. Microsc.* **2005**, *217*, 109–116.
20. Vega, R. A.; Maspoch, D.; Shen, C. K. F.; Kakkassery, J. J.; Chen, B. J.; Lamb, R. A.; Mirkin, C. A. Functional Antibody Arrays through Metal Ion-Affinity Templates. *ChemBioChem* **2006**, *7*, 1653–1657.
21. Cha, T.; Guo, A.; Jun, Y.; Pei, D. Q.; Zhu, X. Y. Immobilization of Oriented Protein Molecules on Poly(ethylene glycol)-Coated Si(111). *Proteomics* **2004**, *4*, 1965–1976.
22. Porath, J.; Carlsson, J.; Olsson, I.; Belfrage, G. Metal Chelate Affinity Chromatography, a New Approach to Protein Fractionation. *Nature* **1975**, *258*, 598–599.
23. Ludden, M. L. W.; Mulder, A.; Schulze, K.; Subramaniam, V.; Tampe, R.; Huskens, J. Anchoring of Histidine-Tagged Proteins to Molecular Printboards: Self-Assembly, Thermodynamic Modeling, and Patterning. *Chem.—Eur. J.* **2008**, *14*, 2044–2051.
24. Wegner, G. J.; Lee, N. J.; Marriott, G.; Corn, R. M. Fabrication of Histidine-Tagged Fusion Protein Arrays for Surface Plasmon Resonance Imaging Studies of Protein−Protein and Protein−DNA Interactions. *Anal. Chem.* **2003**, *75*, 4740–4746.

25. Valiokas, R.; Klenkar, G.; Tinazli, A.; Tampe, R.; Liedberg, B.; Piehler, J. Differential Protein Assembly on Micropatterned Surfaces with Tailored Molecular and Surface Multivalency. *ChemBioChem* **2006**, *7*, 1325–1329.
26. Paborsky, L. R.; Dunn, K. E.; Gibbs, C. S.; Dougherty, J. P. A Nickel Chelate Microtiter Plate Assay for Six Histidine-Containing Proteins. *Anal. Biochem.* **1996**, *234*, 60–65.
27. Piner, R. D.; Zhu, J.; Xu, F.; Hong, S. H.; Mirkin, C. A. "Dip-Pen" Nanolithography. *Science* **1999**, *283*, 661–663.
28. Lee, K. B.; Lim, J. H.; Mirkin, C. A. Protein Nanostructures Formed *via* Direct-Write Dip-Pen Nanolithography. *J. Am. Chem. Soc.* **2003**, *125*, 5588–5589.
29. Noy, A.; Miller, A. E.; Klare, J. E.; Weeks, B. L.; Woods, B. W.; DeYoreo, J. J. Fabrication of Luminescent Nanostructures and Polymer Nanowires Using Dip-Pen Nanolithography. *Nano Lett.* **2002**, *2*, 109–112.
30. Salazar, R. B.; Shovsky, A.; Schonherr, H.; Vancso, G. J. Dip-Pen Nanolithography on (Bio)Reactive Monolayer and Block-Copolymer Platforms: Deposition of Lines of Single Macromolecules. *Small* **2006**, *2*, 1274–1282.
31. Weeks, B. L.; Vaughn, M. W.; DeYoreo, J. J. Direct Imaging of Meniscus Formation in Atomic Force Microscopy Using Environmental Scanning Electron Microscopy. *Langmuir* **2005**, *21*, 8096–8098.
32. Tsien, R. Y. The Green Fluorescent Protein. *Annu. Rev. Biochem.* **1998**, *67*, 509–544.
33. Deng, Y.; Zhu, X. Y.; Kienlen, T.; Guo, A. Transport at the Air/Water Interface Is the Reason for Rings in Protein Microarrays. *J. Am. Chem. Soc.* **2006**, *128*, 2768–2769.
34. Kim, K. H.; Sanedrin, R. G.; Ho, A. M.; Lee, S. W.; Moldovan, N.; Mirkin, C. A.; Espinosa, H. D. Direct Delivery and Submicrometer Patterning of DNA by a Nanofountain Probe. *Adv. Mater.* **2008**, *20*, 330–334.
35. Wu, C. C.; Xu, H. P.; Otto, C.; Reinhoudt, D. N.; Lammertink, R. G. H.; Huskens, J.; Subramaniam, V.; Velders, A. H. Porous Multilayer-Coated AFM Tips for Dip-Pen Nanolithography of Proteins. *J. Am. Chem. Soc.* **2009**, *131*, 7526–7527.
36. Paik, H. J.; Kim, Y. R.; Orth, R. N.; Ober, C. K.; Coates, G. W.; Batt, C. A. End-Functionalization of Poly(3-hydroxybutyrate) *via* Genetic Engineering for Solid Surface Modification. *Chem. Commun.* **2005**, 1956–1958.
37. Luzinov, I.; Julthongpiput, D.; Liebmann-Vinson, A.; Cregger, T.; Foster, M. D.; Tsukruk, V. V. Epoxy-Terminated Self-Assembled Monolayers: Molecular Glues for Polymer Layers. *Langmuir* **2000**, *16*, 504–516.
38. Lu, F. T.; Gao, L. N.; Ding, L. P.; Jiang, L. L.; Fang, Y. Spacer Layer Screening Effect: A Novel Fluorescent Film Sensor for Organic Copper(II) Salts. *Langmuir* **2006**, *22*, 841–845.
39. Stukalov, O.; Murray, C. A.; Jacina, A.; Dutcher, J. R. Relative Humidity Control for Atomic Force Microscopes. *Rev. Sci. Instrum.* **2006**, *77*, 033704.